NACA

RESEARCH MEMORANDUM

LOW-SPEED STATIC LONGITUDINAL AND LATERAL STABILITY

CHARACTERISTICS OF TWO LOW-ASPECT-RATIO WINGS

CAMBERED AND TWISTED TO PROVIDE A UNIFORM

LOAD AT A SUPERSONIC FLIGHT CONDITION

By Lewis R. Fisher

Langley Aeronautical Laboratory
Langley Field, Va.

NATIONAL ADVISORY COMMITTEE
FOR AERONAUTICS
WASHINGTON

June 6, 1951
Declassified December 7, 1953

NATIONAL ADVISORY COMMITTEE FOR AERONAUTICS

RESEARCH MEMORANDUM

LOW-SPEED STATIC LONGITUDINAL AND LATERAL STABILITY

CHARACTERISTICS OF TWO LOW-ASPECT-RATIO WINGS

CAMBERED AND TWISTED TO PROVIDE A UNIFORM

LOAD AT A SUPERSONIC FLIGHT CONDITION

By Lewis R. Fisher

SUMMARY

A delta wing and a tapered, sweptback wing, both of which were cambered and twisted so as to provide a uniform loading at a lift coefficient of 0.2 and a Mach number of 1.62, were investigated in order to determine the low-speed lift-drag and static-stability properties of such wings over the Reynolds number range from 384,000 to 1,550,000. The results of these investigations indicate that the longitudinal stability of the delta wing was almost constant through the lift-coefficient range for the test Reynolds numbers, the swept wing was longitudinally unstable at high lift coefficients, and, in general, the longitudinal stability tended to be somewhat irregular through the lift-coefficient range. The irregularities and the instability at high lift coefficients diminished as the Reynolds numbers were increased, however, and may disappear entirely at full-scale Reynolds numbers.

At low lift coefficients, neither model experienced any important change in directional stability with increasing lift coefficient; at high lift coefficients, however, both models showed a tendency toward increased directional stability.

As the Reynolds number was increased within the range of low values investigated, a scale condition was reached where, because of large increases in the minimum drag and the drag due to lift, the values of the maximum lift-drag ratio were greatly reduced.

INTRODUCTION

In order to minimize compressibility effects at the design lift coefficient, the pressure peaks that usually exist on low–aspect–ratio highly swept wings in supersonic flight can be reduced by incorporating camber and twist into the wing design.

Considerable interest is being shown as well in the effects of camber and twist on the low–speed characteristics of high-speed-wing configurations as a means for delaying leading-edge separation to higher lift coefficients than have been occurring for the plane wing. That this result is accomplished for a 45° sweptback wing of aspect ratio 6 is shown in reference 1.

Two wings designed and constructed to have an approximately uniform lift distribution for a specific supersonic flight condition were tested in the 6- by 6-foot test section of the Langley stability tunnel in order to determine the low–speed lift–drag and static stability characteristics of such wings. The wings tested represent two possible supersonic configurations - a delta wing of aspect ratio 1.56 and leading-edge sweep of 68.7° and a highly tapered (λ = 0.253) sweptback wing of aspect ratio 2.00 and leading-edge sweep of 66.4°. The wings were cambered and twisted in section so as to provide an approximately uniform lift distribution over the wing surface at a lift coefficient of 0.2 and a Mach number of 1.62.

SYMBOLS

The data are presented in the form of standard NACA coefficients of forces and moments which are referred in all cases to the stability axes with the origin at the quarter-chord point of the mean aerodynamic chord of the wings tested. The positive directions of the forces, moments, and angular displacements are shown in figure 1. The coefficients and symbols used herein are defined as follows:

C_L lift coefficient $\left(\dfrac{L}{qS}\right)$

C_D drag coefficient $\left(\dfrac{D}{qS}\right)$

C_Y lateral-force coefficient $\left(\dfrac{Y}{qS}\right)$

C_m pitching-moment coefficient $\left(\dfrac{M}{qS\bar{c}}\right)$

C_l rolling-moment coefficient $\left(\dfrac{L'}{qSb}\right)$

C_n yawing-moment coefficient $\left(\dfrac{N}{qSb}\right)$

L   lift, pounds

D   drag, pounds (D = -X)

X   longitudinal force, pounds

Y   lateral force, pounds

M   pitching moment, foot-pounds

L'   rolling moment, foot-pounds

N   yawing moment, foot-pounds

q   dynamic pressure, pounds per square foot $\left(\frac{1}{2}\rho V^2\right)$

ρ mass density of air, slugs per cubic foot

V   free-stream velocity, feet per second

S   wing area, square feet

b   wing span, feet

A   aspect ratio $\left(\dfrac{b^2}{S}\right)$

λ taper ratio

c   local streamwise chord of wing, feet

$\bar{c}$ mean aerodynamic chord, feet $\left(\dfrac{2}{S}\displaystyle\int_0^{b/2} c^2 \, dy\right)$

t   thickness of wing section, feet

x   longitudinal distance from wing apex to coordinate origin, feet

x'   longitudinal distance from wing apex to any point on wing, feet

y   distance measured perpendicular to plane of symmetry, feet

$\bar{y}$ distance from plane of symmetry to mean aerodynamic chord, feet

z vertical distance from XY-plane to wing mean camber line, feet

z' camber, feet

R Reynolds number $\left(\dfrac{\rho V \bar{c}}{\mu}\right)$

μ coefficient of viscosity of air, pounds per foot-second

M Mach number $\left(\dfrac{V}{a}\right)$

a local velocity of sound, feet per second

α angle of attack, degrees

ψ angle of yaw, degrees

ϵ angle of twist at any spanwise station measured with respect to fuselage center line, degrees

$$C_{L_\alpha} = \frac{\partial C_L}{\partial \alpha}$$

$$C_{l_\psi} = \frac{\partial C_l}{\partial \psi}$$

$$C_{n_\psi} = \frac{\partial C_n}{\partial \psi}$$

$$C_{Y_\psi} = \frac{\partial C_Y}{\partial \psi}$$

APPARATUS AND TESTS

The two low-aspect-ratio wings tested were cambered and twisted so as to provide an approximately uniform load distribution in both the spanwise and chordwise planes at a lift coefficient of 0.2 and a Mach number of 1.62. One wing had a delta plan form of aspect ratio 1.56. The second wing was a highly tapered sweptback wing having an aspect ratio of 2.00 and a leading edge swept back 66.4°. Details of the models are given in figure 2. Photographs of the models mounted in the 6- by 6-foot test section of the Langley stability tunnel are shown in figure 3. The

spanwise distributions of twist, camber, and thickness are indicated in
figure 4. The angle of twist is measured with respect to the fuselage
center line. The wing-root sections of both models were NACA 0002
profiles. Both wings were constructed of mahogany and were tested in
combination with a fuselage which was a body of revolution with a fineness
ratio of about 10.

The models were mounted at the quarter-chord point of the mean aero-
dynamic chord for each wing on the single strut support shown in figure 3.
All forces and moments were measured about that point by a conventional
six-component balance. A dummy support strut was used in order to
determine the tares due to the support strut.

The test conditions for both models are tabulated as follows:

Dynamic pressure, q (lb/sq ft)	Mach number, M	Reynolds number, R	
		Delta wing	Swept wing
4.0	0.05	491,000	384,000
16.0	.10	983,000	768,000
24.9	.13	1,226,000	958,000
39.8	.17	1,550,000	1,212,000

The Reynolds numbers are based on the mean aerodynamic chord for each
wing.

Both models were tested through an angle-of-attack range from -4°
to 32° for each of the three lowest dynamic pressures. At a dynamic
pressure of 39.8 pounds per square foot, because of strength limitations
of the models, the upper limits of the angle-of-attack range were 20°
and 22° for the delta wing and the swept wing, respectively. The angle
of attack was measured with respect to the fuselage center line. At a
dynamic pressure of 24.9 pounds per square foot, both models were also
tested through the angle-of-attack range at angles of yaw of $\pm 5^\circ$ in order
to determine the lateral-stability derivatives.

CORRECTIONS

The angle of attack, drag coefficient, and rolling-moment coefficient
have been corrected for jet-boundary effects by means of the usual
unswept-wing theory.

Inasmuch as it was not expected that Reynolds number should have any important effect on the tare values for lift, drag, and pitching moment, these tares were determined only at the Reynolds number corresponding to a dynamic pressure of 24.9 pounds per square foot. The faired values of the tares were then applied to the lift, drag, and pitching-moment data for all Reynolds numbers. No tare corrections were made for the lateral-force coefficient, rolling-moment coefficient, or yawing-moment coefficient. No corrections were made for any effects of blocking which are believed to be negligible. All Reynolds numbers indicated are test Reynolds numbers.

RESULTS AND DISCUSSION

The aerodynamic characteristics in pitch for both models tested at each of four Reynolds numbers are presented in figure 5, and the lift-drag ratios based on these data are shown in figure 6. The effect of increasing Reynolds number upon the lift-curve slopes, the minimum drag coefficient, and the maximum lift-drag ratio are summarized in figure 7. The static-lateral-stability properties of the models are shown in figure 8.

Longitudinal Characteristics

For both models, the lift, drag, and pitching-moment curves, shown in figure 5, exhibit trends which appear to be characteristic of cambered and twisted wings at low Reynolds numbers. At a low lift coefficient, and for all Reynolds numbers, the models experienced a transitory decrease in lift-curve slope, through a short lift-coefficient range, after which recovery to approximately the original lift-curve slope was made. The change in slope was less extreme for the delta wing than for the swept wing. In general, the delta wing exhibited more uniform lift curves through the lift-coefficient range at all Reynolds numbers than did the swept wing. An increase in Reynolds number for each wing appeared to increase the uniformity of the lift curves. The effect of Reynolds number on the lift-curve slopes at zero lift and the minimum-drag coefficients for both models are summarized in figure 7. At all Reynolds numbers, the swept wing (A = 2.00) gives higher values of C_{L_α} than does the delta wing (A = 1.56), but for each wing the variation of C_{L_α} with Reynolds number is small. The minimum drag coefficients over the lower range of Reynolds numbers are generally smaller than at higher Reynolds numbers. In general, the swept wing exhibits lower values of the minimum drag coefficient than does the delta wing.

The variations with lift coefficient of the lift-drag ratios for both wings at the Reynolds numbers at which tests were made appear in figure 6. The maximum L/D for each scale condition occurs at about the design lift coefficient of 0.2 for both wings. At lift coefficients higher than 0.6, Reynolds number had no effect on the lift-drag ratio.

A definite variation with Reynolds number takes place for the maximum values of the lift-drag ratio. This trend may be seen in the lower portion of figure 7. For both wings, a particular Reynolds number is reached where a transition apparently occurs from laminar to turbulent boundary-layer flow. At Reynolds numbers of 1.1×10^6 for the delta wing and 0.9×10^6 for the swept wing, a sharp reduction, by a factor of about two, in the values of $(L/D)_{max}$ takes place. Although no considerable emphasis should be placed on these very low Reynolds number data, it should be pointed out that the reduction in $(L/D)_{max}$ is attributed to an increase in the drag due to lift of the wings as well as to an increase in the drag at zero lift. The over-all values of $(L/D)_{max}$ for the swept wing are appreciably higher than those for the delta wing, and the change in $(L/D)_{max}$ with Reynolds number is greater for the swept wing than for the delta wing.

The pitching-moment curves for the delta wing are linear through the lift-coefficient range. The aerodynamic center is at the $0.41\bar{c}$ point at zero lift and does not shift appreciably with a change in Reynolds number. The pitching-moment curves for the swept wing are somewhat irregular in slope and signify static longitudinal instability at the higher lift coefficients. The trend is for the instability to diminish at the high Reynolds numbers, however. It is possible that at full-scale Reynolds numbers, the instability will disappear at least for the lift-coefficient range in which it now appears. At zero lift, the aerodynamic center is at $0.39\bar{c}$ for the swept wing and it does not vary appreciably with Reynolds number.

Lateral Characteristics

The static-lateral-stability derivatives for the two models appear in figure 8. The values of the effective dihedral parameter C_{l_β} $\left(\text{where } C_{l_\beta} = -C_{l_\psi}\right)$ for the swept wing are greater than those for the delta wing through the lower portion of the lift-coefficient range. At higher lift coefficients, the delta wing has the higher effective dihedral. The slope $\left(\dfrac{\partial C_{l_\psi}}{\partial C_L}\right)_{C_L \rightarrow 0}$ is slightly greater for the delta wing than it is for the swept wing.

Up to a lift coefficient of about 0.4, there is no variation of the directional-stability parameter C_{n_ψ} with lift coefficient for either model. Since at low lift coefficients the swept-wing model is slightly less unstable than the delta-wing model, and at high lift coefficients it has less directional stability than the delta-wing model, the net change in directional stability is smaller for the swept-wing model than for the delta-wing model. Both wings show a tendency toward increased directional stability at high lift coefficients.

The delta-wing model produced higher values of the lateral force due to sideslip C_{Y_ψ} than did the swept-wing model at practically all lift coefficients. At low lift coefficients, C_{Y_ψ} changed very little with lift coefficient for either model.

CONCLUSIONS

The following conclusions were drawn from the results of an experimental investigation of the low-speed static longitudinal and lateral characteristics of two wings which were cambered and twisted to provide a uniform load at a supersonic flight condition:

1. The delta-wing model exhibited almost constant static longitudinal stability through the lift-coefficient range at all Reynolds numbers at which tests were made. The lift and pitching-moment data for the swept wing were somewhat irregular, but these irregularities became less severe as the Reynolds number increased. At high lift coefficients, the swept wing was longitudinally unstable, but the instability diminished at higher Reynolds numbers. It is possible that at full-scale Reynolds numbers, the irregularities and the instability indicated by the data for the swept wing may disappear.

2. Neither model tested showed any important variation of the directional stability with lift coefficient in the low-lift-coefficient range. Both models, however, exhibited a tendency toward increased directional stability at high lift coefficients. The swept-wing model had more effective dihedral and less directional instability at low lift coefficients than the delta-wing model. At high lift coefficients, the swept-wing model showed less effective dihedral and less directional stability than the delta-wing model.

3. As the Reynolds number is increased within the range of low values investigated, the values of the maximum lift-drag ratio are greatly reduced because of large increases in the minimum drag and the drag due to lift. The maximum lift-drag ratios at all Reynolds numbers occurred at about the design lift coefficient for both wings.

Langley Aeronautical Laboratory
    National Advisory Committee for Aeronautics
        Langley Field, Va.

REFERENCE

1. Hunton, Lynn W.: Effects of Twist and Camber on the Low-Speed
    Characteristics of a Large-Scale 45° Swept-Back Wing. NACA
    RM A50A10, 1950.
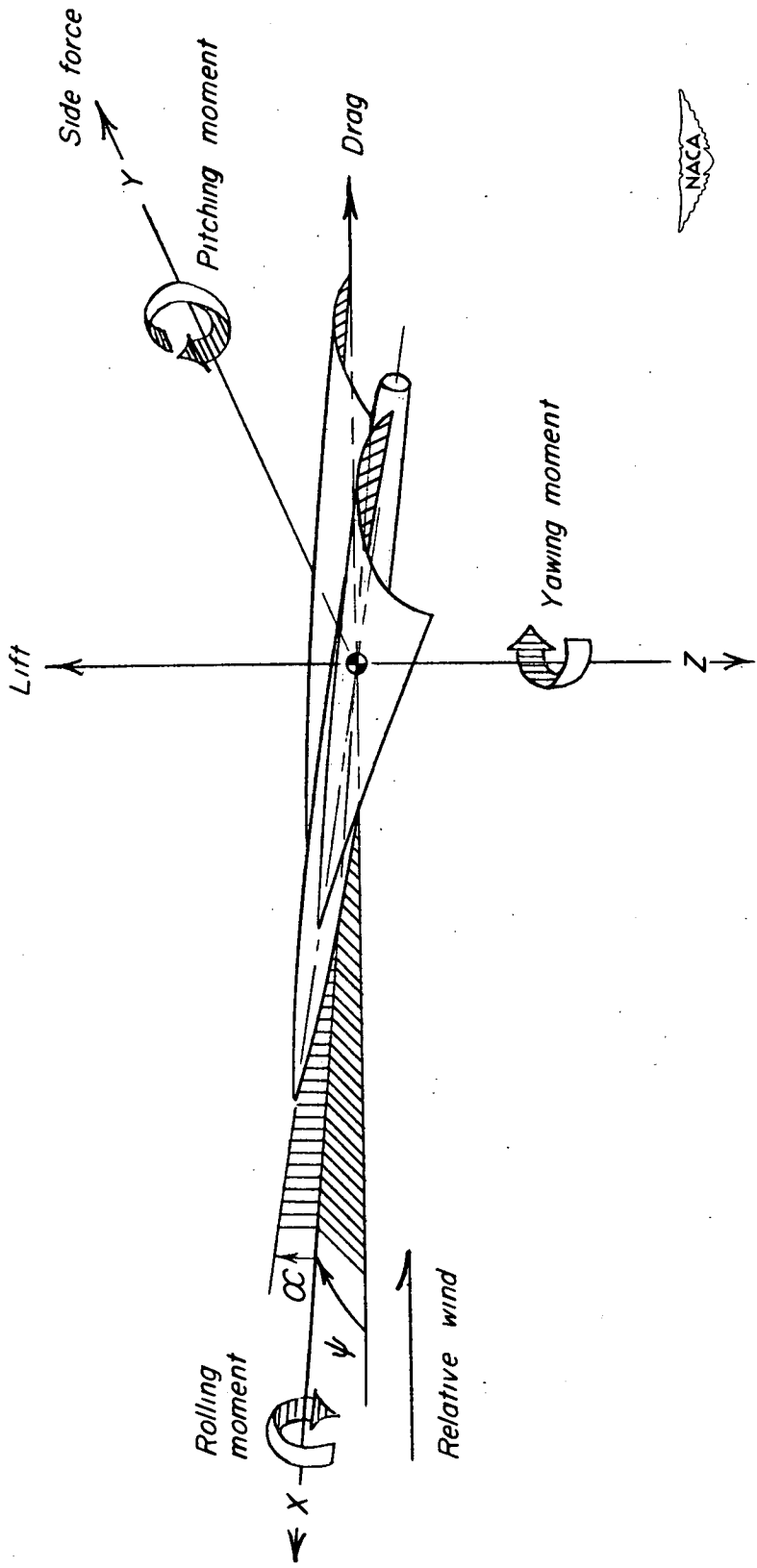
Figure 1.- System of stability axes. Arrows indicate positive direction of angles, forces, and moments.

	Delta Wing	Swept Wing
Aspect ratio	1.56	2.00
Wing span, feet	1.56	1.86
Wing area, square feet	1.56	1.74
Angle of sweep, L.E., degrees	68.7	66.4
Root chord, feet	2.02	1.48
Tip chord, feet	0	0.38
Taper ratio	0	.253
Mean aerodynamic chord, feet	1.33	1.04
C.G. location, x, feet	1.01	1.12
M.A.C. location, $\bar{y}$, feet	0.26	0.38
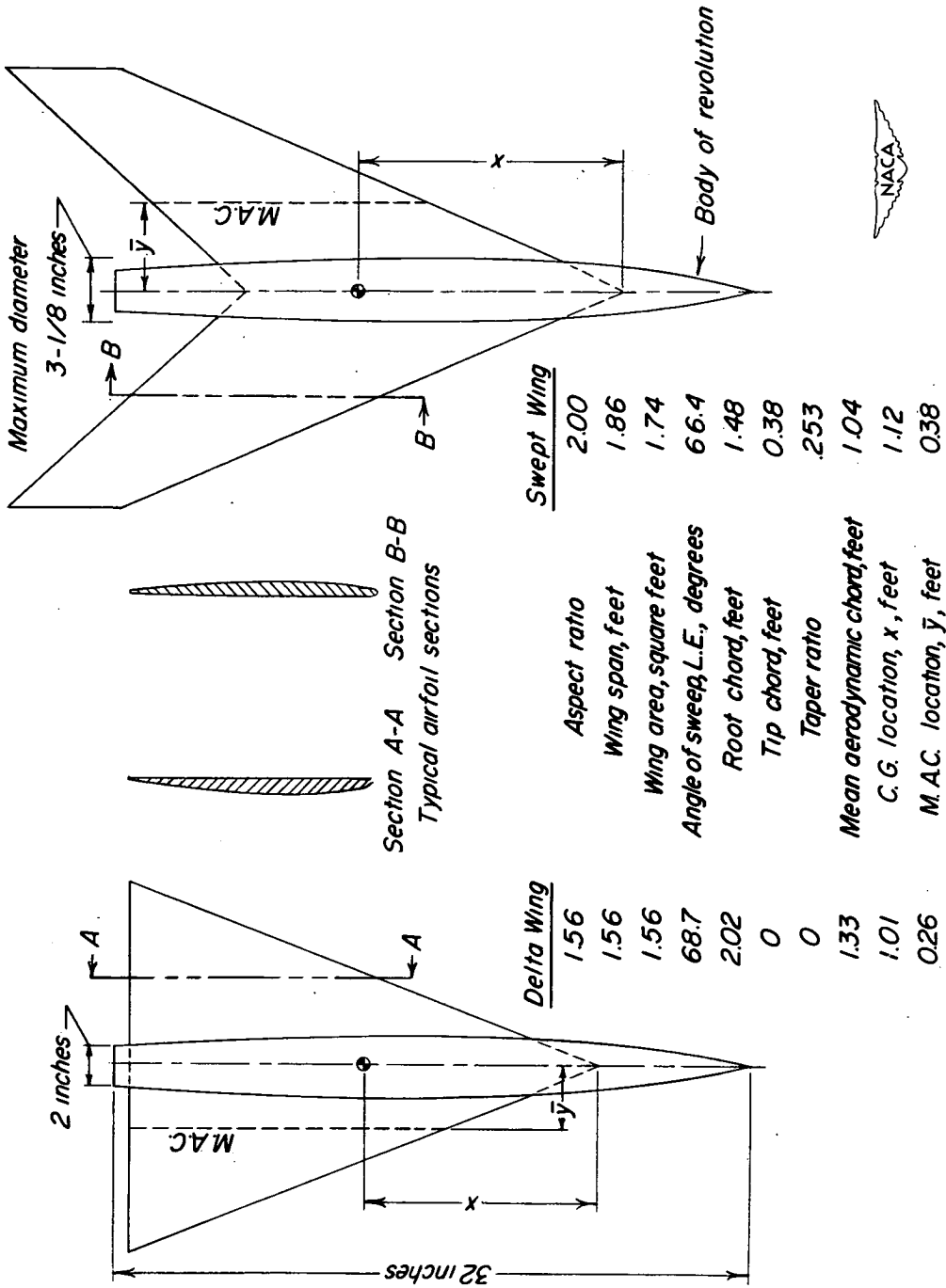
Figure 2.- Plan forms and geometric characteristics of two wings cambered and twisted so as to provide uniform chordwise and spanwise lift distributions at a specific lift coefficient and supersonic Mach number.
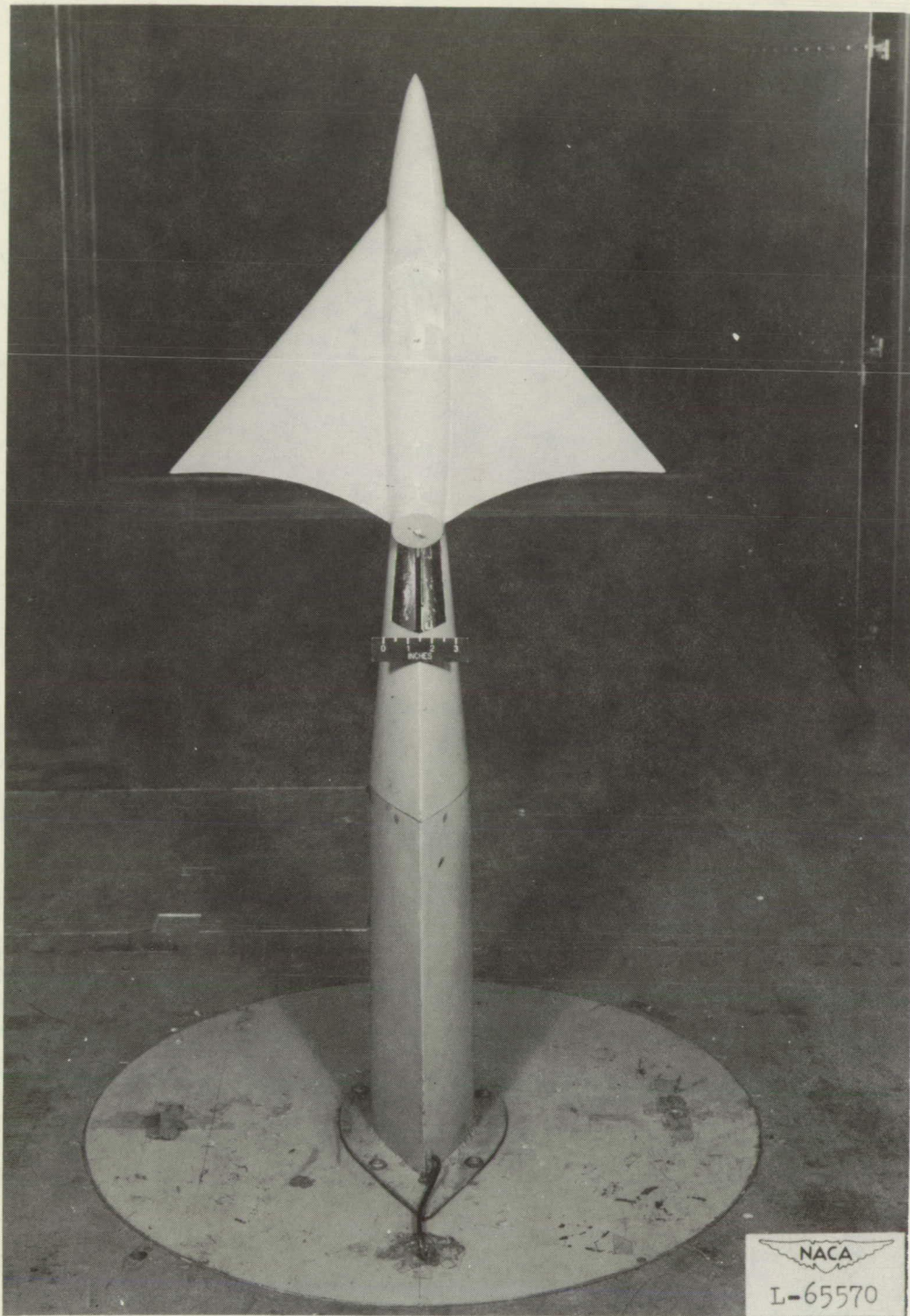
(a) Delta wing, top rear view.

Figure 3.- Cambered and twisted wings mounted in the Langley stability
tunnel.
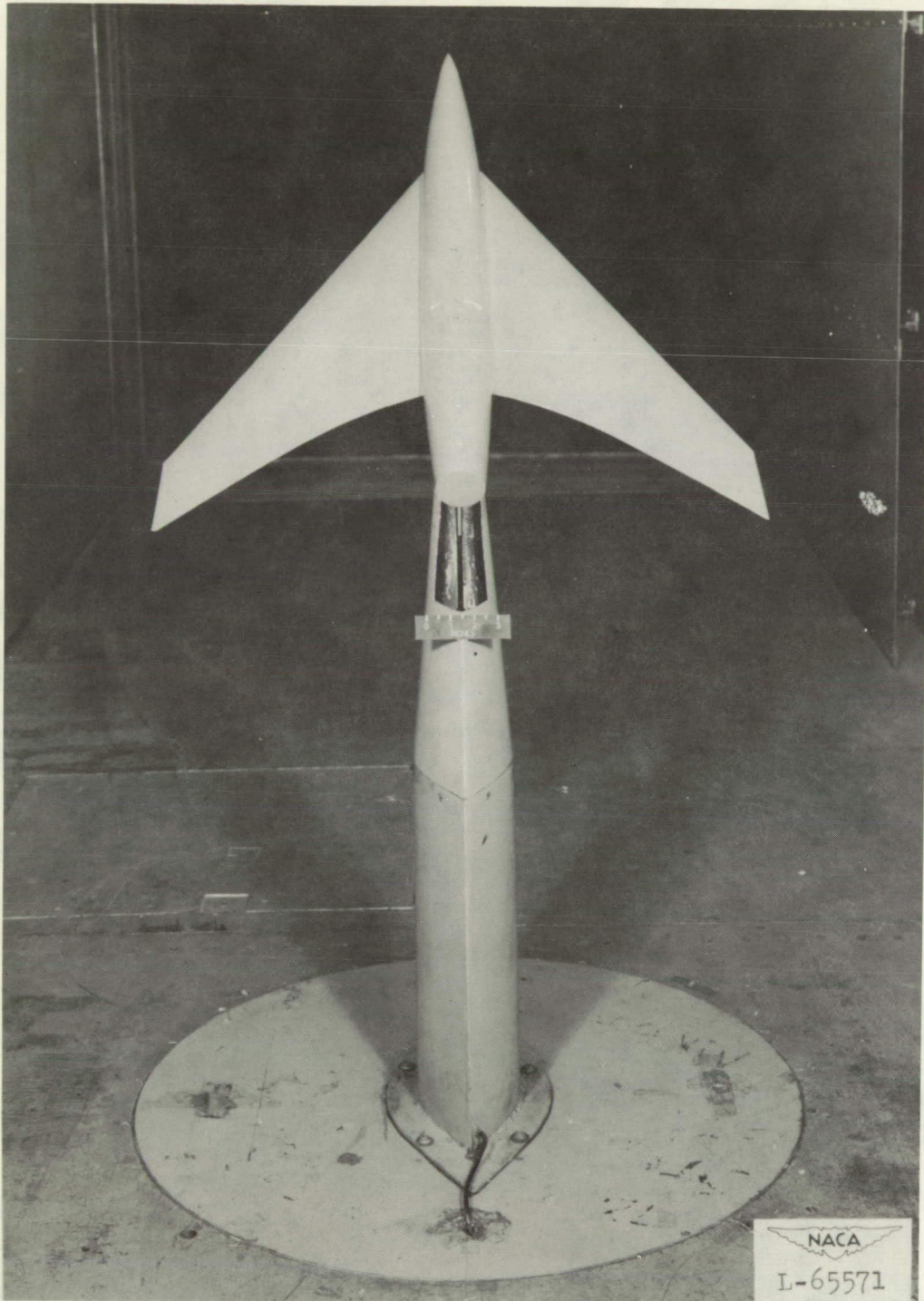
(b) Swept wing, top rear view.

Figure 3.- Continued.
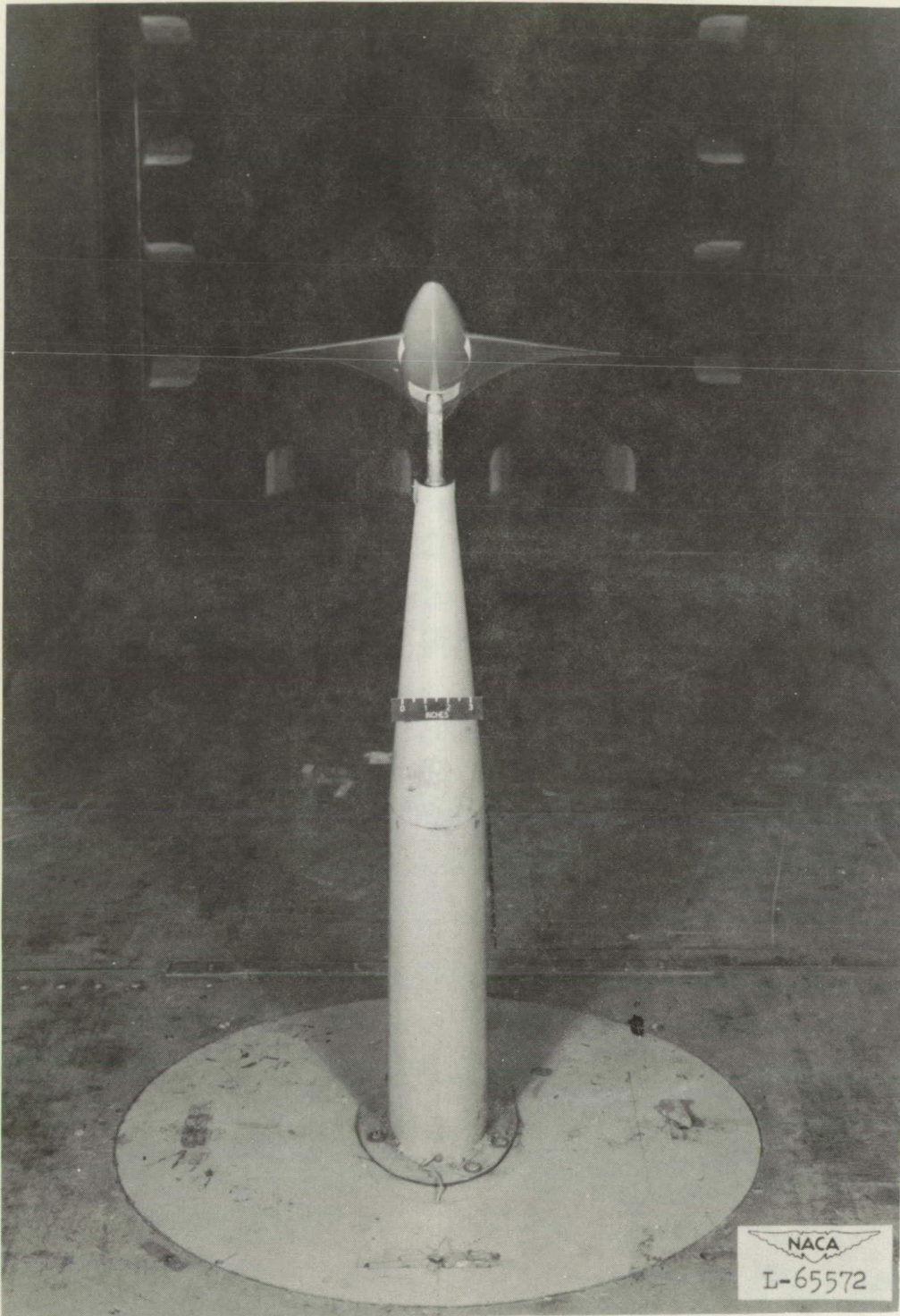
(c) Delta wing, front view.

Figure 3.- Concluded.
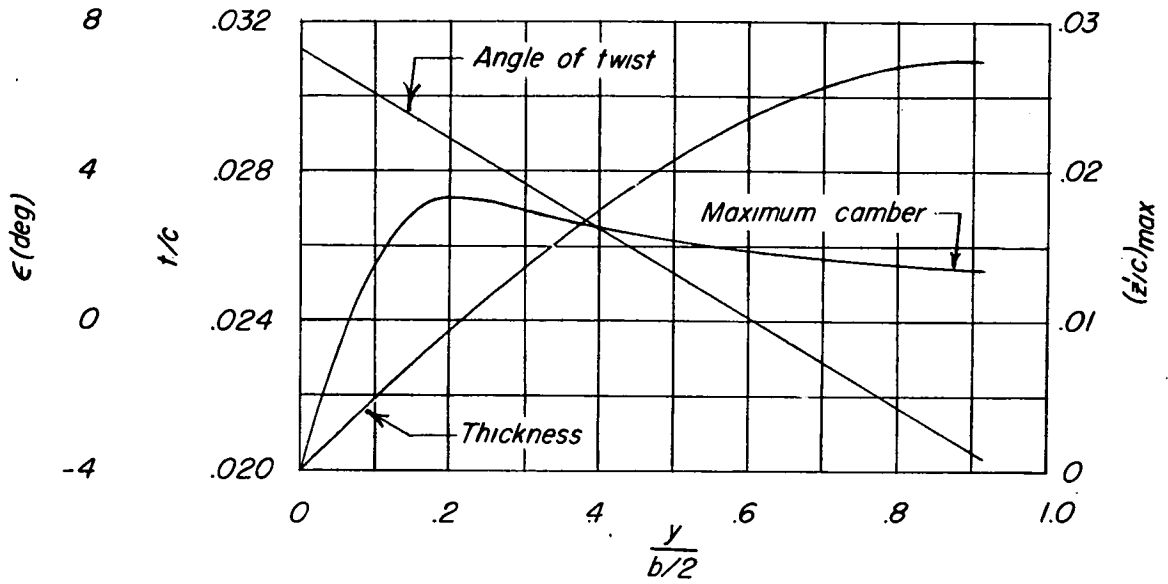
(a) Spanwise distributions of angle of twist, thickness ratio, and
maximum camber.
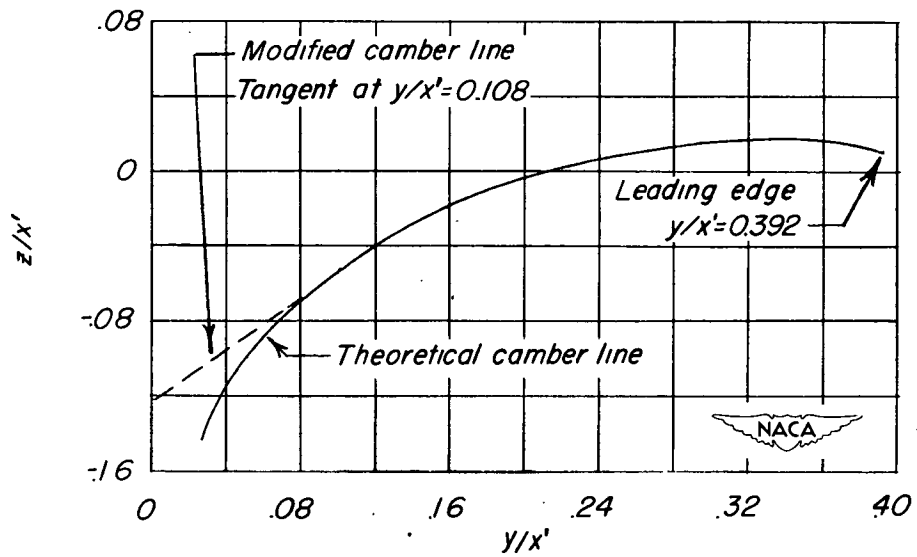
(b) Relative distance of mean camber surface above XY-plane.

Figure 4.- Design details of wings tested.
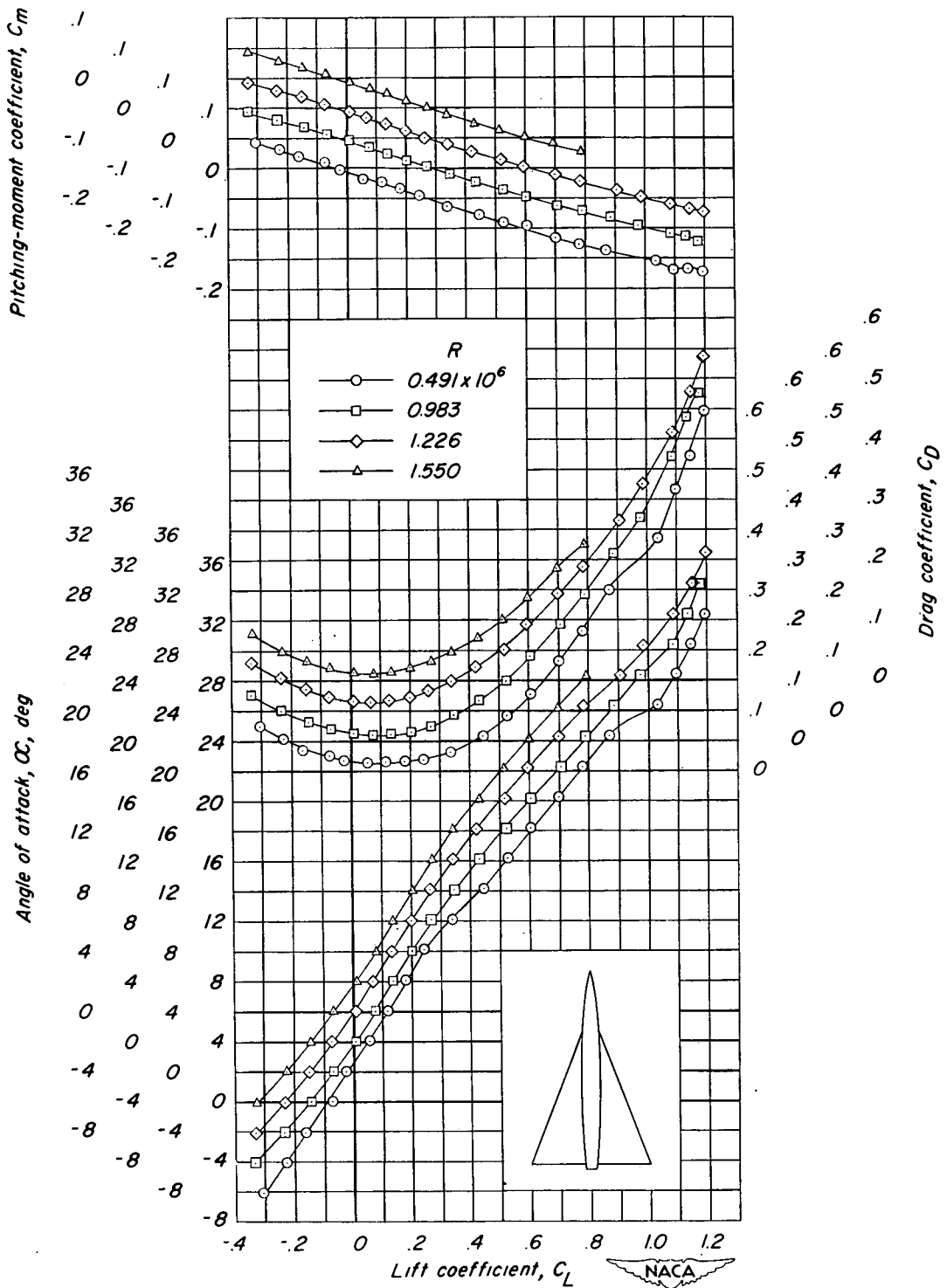
(a) Delta wing.

Figure 5.- Aerodynamic characteristics of two cambered and twisted wings.
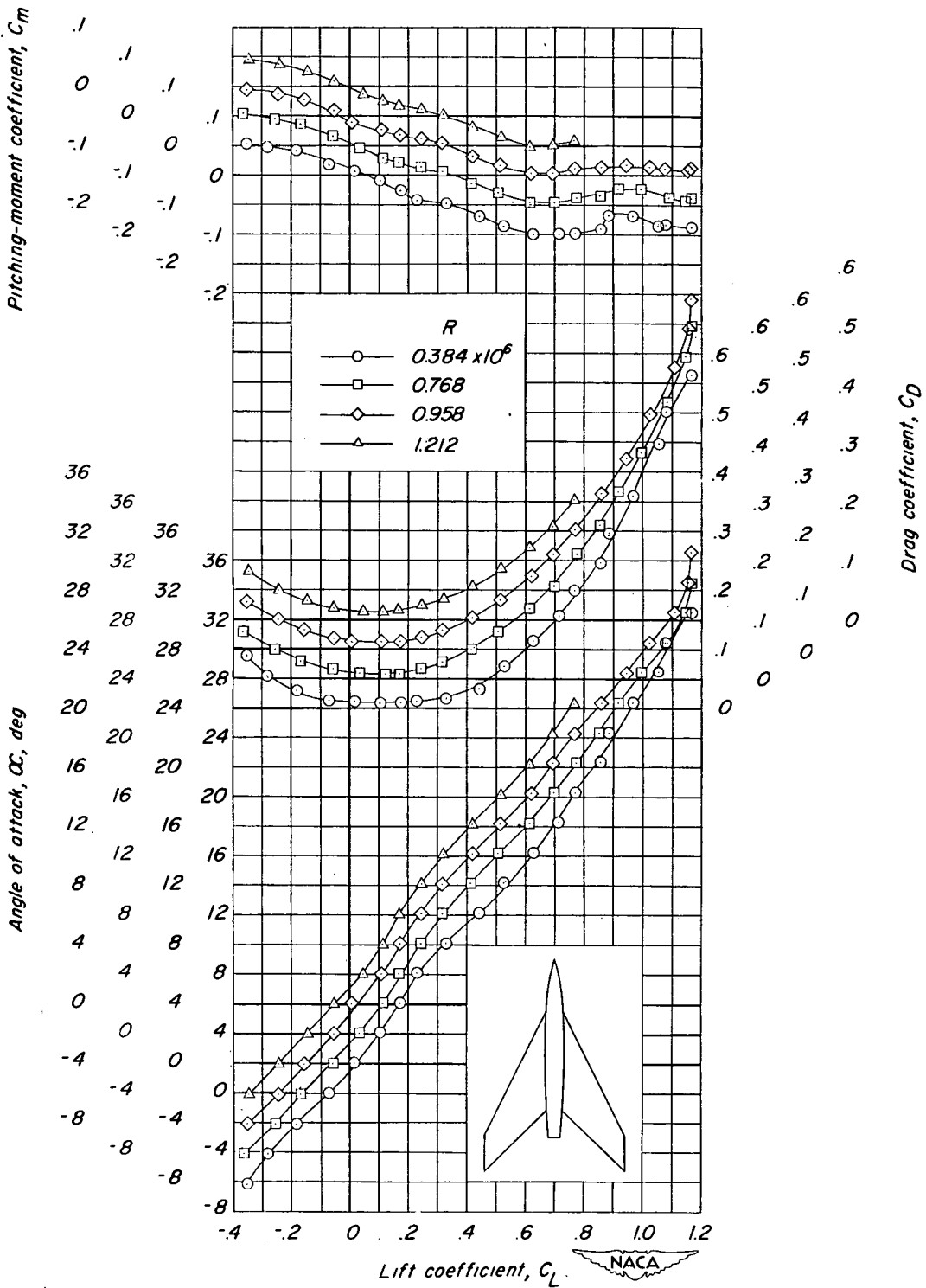
(b) Swept wing.

Figure 5.- Concluded.
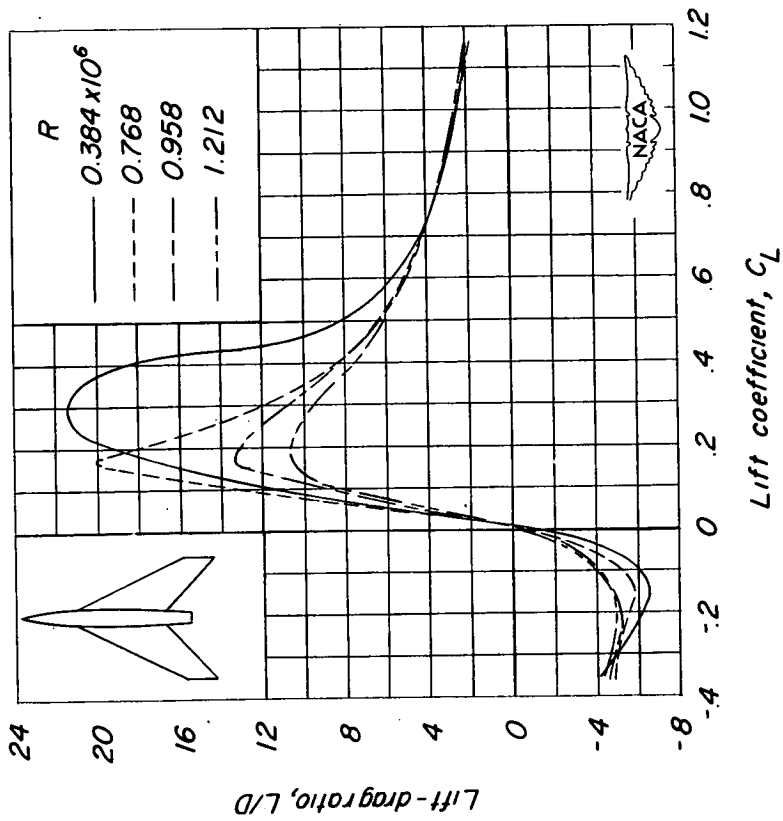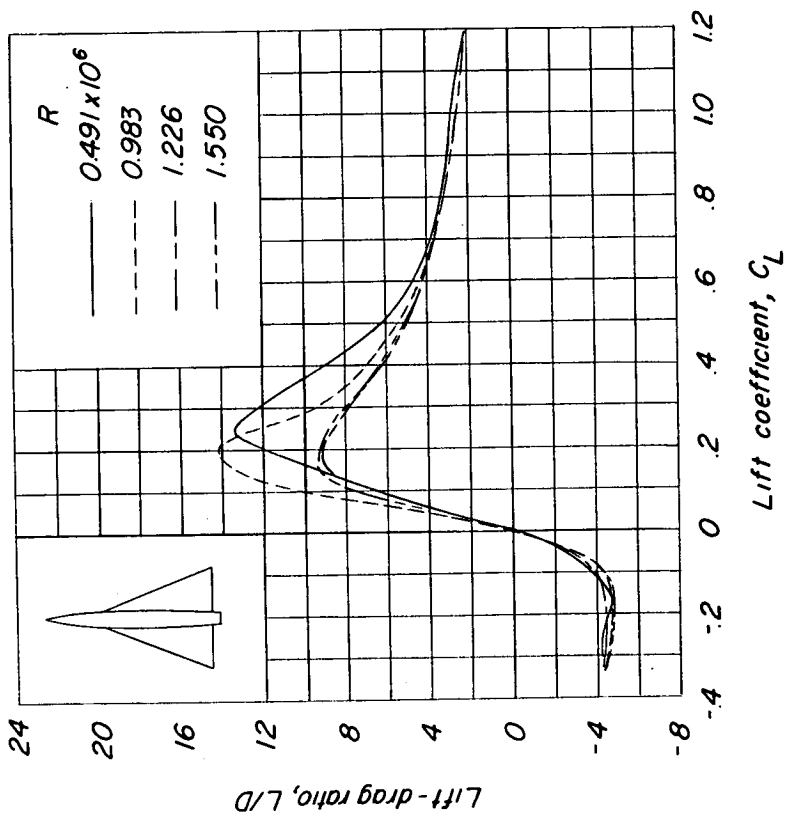
(b) Swept wing.

(a) Delta wing.

Figure 6.- Variation with lift coefficient of lift-drag ratios of two cambered and twisted wings for four Reynolds numbers.
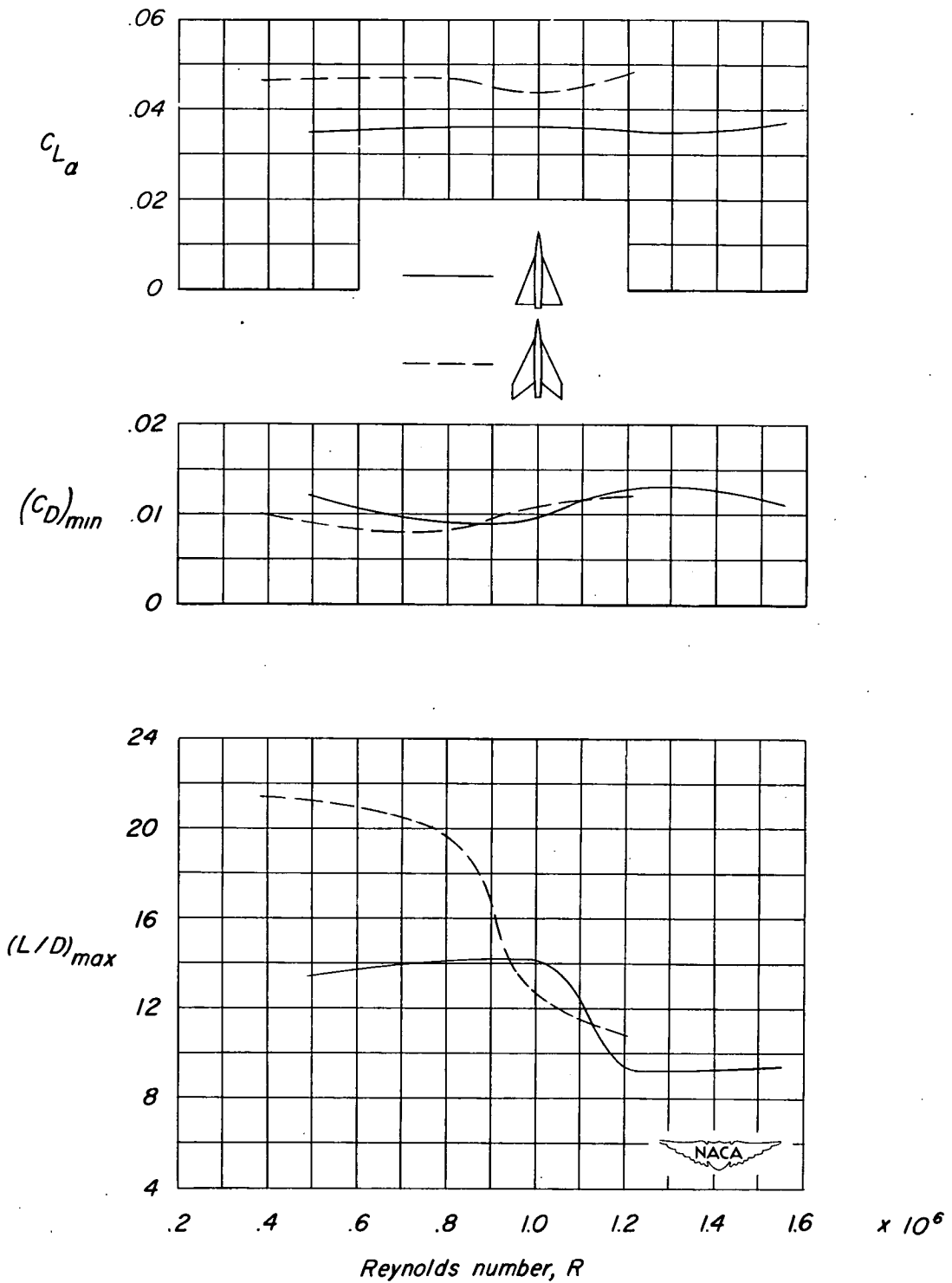
Figure 7.- The variation with Reynolds number of the lift-curve slope, minimum drag coefficient, and maximum lift-drag ratio for two cambered and twisted wings.
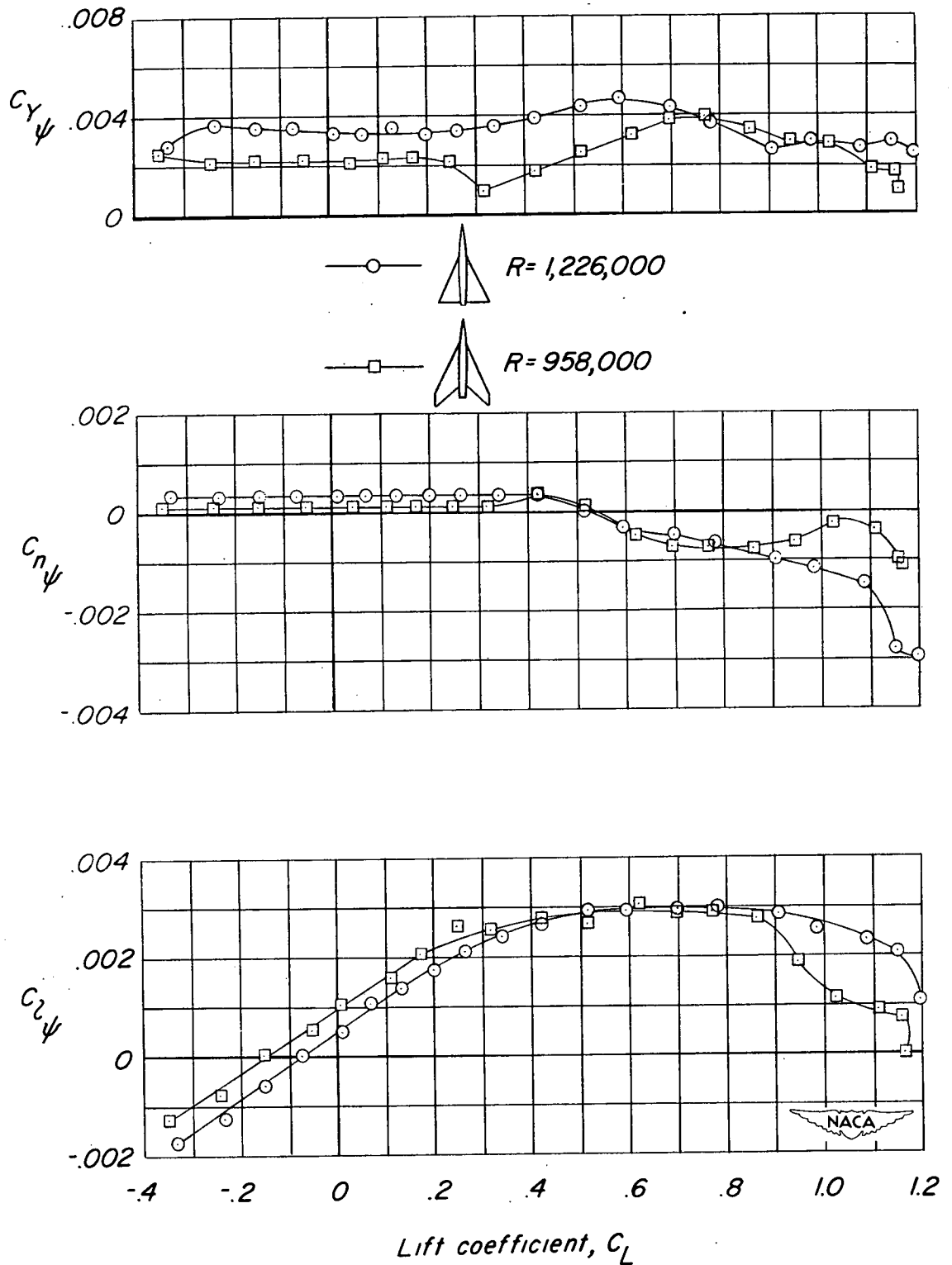
Figure 8.- Lateral static stability characteristics of two cambered and twisted wings.